Electronic Supplementary Material (ESI) for Chemical Communications

Supporting Information for: Molecular Polarization Bridging Physical and Chemical Enhancements in Surface Enhanced Raman Scattering

Sai Duan,[a,b] Xin Xu,*[c] Yi Luo*[b] and Zhong-Qun Tian[a]

[a] *State Key Laboratory of Physical Chemistry of Solid Surface and Department of Chemistry, College of Chemistry and Chemical Engineering, Xiamen University, Xiamen, 361005, P. R. China*
[b] *Department of Theoretical Chemistry, School of Biotechnology, Royal Institute of Technology, S-106 91 Stockholm, Sweden. Fax: +46 (0)8 55378590; Tel: +46 (0)8 55378414; E-mail: luo@kth.se*
[c] *MOE Laboratory for Computational Physical Science, Department of Chemistry, Fudan University, Shanghai, 200433, P. R. China. Fax: +86 (0)21 65643529; Tel: +86 (0)21-65642032; E-mail: xxchem@fudan.edu.cn*

S1 Basic Theory

As discussed in the text, calculations of the actual electric field F^i felt by the adsorbed molecule and the derivatives of polarizabilities $\partial\alpha^i / \partial Q$ where the molecule is interacting with the substrate under the SERS environment are critical issues to properly address the SERS enhancement mechanisms. Here we introduce a practical computational approach to calculate F^i and $\partial\alpha^i / \partial Q$, which can be conveniently applied to real molecular systems such as those shown in Fig. S1.

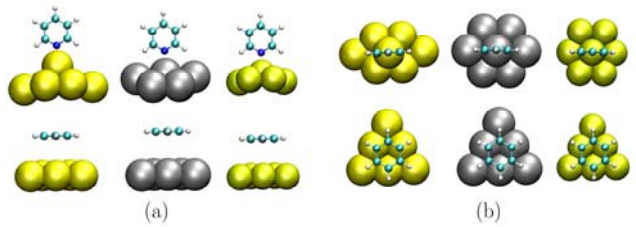

Fig. S1 Optimized geometries of pyridine (top) and benzene (bottom) adsorbed on gold, silver, and copper substrates, from left to right, at the B3LYP/Sadlej pVTZ/Lanl2dz level. (a) side view and (b) top view.

It shall be noted that these issues related to SERS actually share their common origin with the classical local field factor problem in linear and nonlinear optics.[1, 2] In the latter case, a general computational approach with Onsager model for calculating polarizabilities and their derivatives has already been established.[2] We will first briefly recapture the method in the following in terms of SERS enhancement factor calculations.

In general, we could add solvation energy $-\frac{1}{2}\sum_{mn} f^R_{mn}\mu_m\mu_n$, where $m,n \in \{x,y,z\}$, of the Onsager model as the long range interaction energy between the adsorbate molecule and the substrate into the molecular polarizability calculations. Thus, if we neglect the contribution of hyperpolarizabilities, properties in the presence of SERS environment could be calculated as[1]

$$\begin{aligned} \mu^i &= \mu^{Loc} \\ F^R &= f^R \mu^{Loc} \\ \alpha^i &= \left(\mathrm{I} - f^R \alpha^{Loc}\right)^{-1} \alpha^{Loc} \end{aligned} \tag{1.1}$$

where superscript "*i*" represents molecular properties under the SERS environment. Superscript "*Loc*" represents the extracted molecular properties from metal-molecule complex system, which contain only the short range chemical interaction. Superscript "*R*" represents properties generated by the polarization of the molecule. Here f^R denotes reaction field factor matrix in Onsager model and is given by[3]

$$f^R_{mn} = \frac{3}{a_x a_y a_z} \frac{\kappa_m(1-\kappa_m)(\epsilon_2-\epsilon_1)}{\epsilon_2 + (\epsilon_1-\epsilon_2)\kappa_m} \delta_{mn} \tag{1.2}$$

where δ_{mn} is a δ function, a_x, a_y, and a_z the principal axes of an ellipsoidal cavity, ϵ_2 the dielectric constant of bulk metal at the incident light wavelength, ϵ_1 the dielectric constant of the solution around molecules, and κ_m is defined as[3]

$$\kappa_m = \frac{a_x a_y a_z}{2} \int_0^\infty \left[\left(s+a_x^2\right)\left(s+a_y^2\right)\left(s+a_z^2\right)\right]^{-1/2} \left(s+a_m^2\right)^{-1} \mathrm{d}s \tag{1.3}$$

In our calculations, the experimental dielectric constants for metals are employed for ϵ_2 and permittivity of vacuum is used for ϵ_1.[4] We use spherical cavity for simplicity in the present work. The detailed calculations for molecular polarizabilities at such a semi-classical level, as well as the comparison with the exact self-consistent reaction filed (SCRF) results are given in section **S3**.

The relationship between the actual electric field F^i felt by the adsorbed molecule and the field from the surface plasmon F^P induced by the incident light is $F^i = F^P + F^R$, where F^R is the reaction field generated by the polarization of the molecule. F^i and F^P are related in Onsager model by[3]

$$F^i = \left(\mathrm{I} - f^R \alpha^i\right)^{-1} F^P \tag{1.4}$$

When no molecules are present, F^i and F^P are equivalent.

This indicates that the electric field obtained from the conventional finite-difference time-domain (FDTD) method is F^P, and it should be corrected by a physical coupling factor (G_{Coup}^{Phys}) when calculating electric field enhancement of incident light,

$$G_{Coup}^{Phys} = \frac{\left|F^i\right|^2}{\left|F^P\right|^2} \tag{1.5}$$

Since electric field of the incident light is perpendicular to the metal surface, F^P only has its z component. Hence, G_{Coup}^{Phys} is calculated by

$$G_{Coup}^{Phys} = \left|\left(\mathrm{I} - f^R \alpha^i\right)_{zz}^{-1}\right|^2 \tag{1.6}$$

Raman scattering factors are calculated as usual[5]

$$S_k = 45a_k'^2 + 7\gamma_k'^2 \tag{1.7}$$

where

$$a_k' = \frac{1}{3}\left[\left(\bar{\alpha}_{xx}'\right)_k + \left(\bar{\alpha}_{yy}'\right)_k + \left(\bar{\alpha}_{zz}'\right)_k\right]$$

$$\gamma_k'^2 = \frac{1}{2}\left\{\begin{array}{l}\left[\left(\bar{\alpha}_{xx}'\right)_k - \left(\bar{\alpha}_{yy}'\right)_k\right]^2 + \left[\left(\bar{\alpha}_{yy}'\right)_k - \left(\bar{\alpha}_{zz}'\right)_k\right]^2 \\ + \left[\left(\bar{\alpha}_{zz}'\right)_k - \left(\bar{\alpha}_{xx}'\right)_k\right]^2 + 6\left[\left(\bar{\alpha}_{xy}'\right)_k^2 + \left(\bar{\alpha}_{yz}'\right)_k^2 + \left(\bar{\alpha}_{zx}'\right)_k^2\right]\end{array}\right\}$$

$$\left(\bar{\alpha}_{rs}'\right)_k = \left(\frac{\partial \bar{\alpha}_{rs}}{\partial Q_k}\right)_0 \tag{1.8}$$

From the relationship between α^i and α^{Loc} in Eq. (1.1), we can obtain the derivative of α^i as

$$\begin{aligned}\alpha^{i\prime} = &\left(\mathrm{I} - f^R\alpha^{Loc}\right)^{-1} f^R \alpha^{Loc\prime}\left(\mathrm{I} - f^R\alpha^{Loc}\right)^{-1}\alpha^{Loc} \\ &+\left(\mathrm{I} - f^R\alpha^{Loc}\right)^{-1}\alpha^{Loc\prime}\end{aligned} \tag{1.9}$$

To obtain Eq. (1.9), we have assumed an independence of f^R with small nuclei motion. Once $\left(\bar{\alpha}_{rs}^{i\prime}\right)_k$ is obtained, the Raman scattering factors with long range interaction correction can be calculated by the same definition as in Eq. (1.7). The chemical part (G_{Coup}^{Chem}) in the coupling enhancement (G_{Coup}) is thus defined as

$$G_{Coup,k}^{Chem} = \frac{S_k^i}{S_k^{Loc}} \tag{1.10}$$

S2 Configurations for Pyridine and Benzene Adsorbed on Coinage Metal Substrates

Our strategy is to use cluster models to first consider the local chemical interactions between adsorbate molecule and substrate and then to include the long range interaction through the reaction filed theory. We take the initial adsorption geometries from the periodic boundary condition calculations where pyridine (py) and benzene (ben) are adsorbed on the face-centered cubic (FCC) (111) surfaces of gold, silver, and copper, respectively.[6, 7] Py-metal and Ben-metal complexes are restricted in the C_{2V} and C_{3V} symmetries, respectively. Full geometry optimizations are performed at the B3LYP level in conjunction with the Sadlej pVTZ basis sets[8] for carbon, nitrogen and hydrogen atoms and the Lanl2dz basis set for metal atoms as implemented in the Gaussian 03 suite of programs.[9] The optimized structures are depicted in Fig. S1. Analytical vibrational frequency calculations are carried out and Raman intensity calculations of all complexes are also performed at the same level. As noted before, small imaginary frequencies may exist, which were attributed to the integral errors in density functional theory calculations.[10]

S3 Calculations of Polarizabilities of Adsorbate Molecules

The polarizabilities α_{ab} can be calculated as[11]

$$\alpha_{ab} = \frac{\partial^2 E(tot)}{\partial F_a \partial F_b} \tag{1.11}$$

where $E(tot)$ is the total energy of the whole complex system and F_a and F_b are the external electric fields along the *a* and *b* directions, respectively. We may decompose $E(tot)$ of a metal-molecule complex system into three terms as

$$E(tot) = E_{\mathrm{Metal}} + E_{\mathrm{Mol}} + E_{\mathrm{Int}} \tag{1.12}$$

where E_{Metal} denotes the energy calculated with the metal fragment alone, and E_{Mol} the energy calculated with the molecular fragment alone. We assume E_{Int}, the energy difference between $E(tot)$ and ($E_{\mathrm{Metal}} + E_{\mathrm{Mol}}$), to be the interaction energy between metal and the molecular fragment in the complex. Hence the polarizabilities α_{ab} of a metal-molecule complex system may be decomposed as

$$\alpha_{ab} = \alpha_{ab}^{\mathrm{Metal}} + \alpha_{ab}^{\mathrm{Mol}} \tag{1.13}$$

where $\alpha_{ab}^{\mathrm{Metal}} = \frac{\partial^2 E_{\mathrm{Metal}}}{\partial F_a \partial F_b} + \frac{1}{2}\frac{\partial^2 E_{\mathrm{Int}}}{\partial F_a \partial F_b}$ and $\alpha_{ab}^{\mathrm{Mol}} = \frac{\partial^2 E_{\mathrm{Mol}}}{\partial F_a \partial F_b} + \frac{1}{2}\frac{\partial^2 E_{\mathrm{Int}}}{\partial F_a \partial F_b}$. In the conventional molecule-metal cluster model, only short range local chemical bond interaction is properly included in $\alpha_{ab}^{\mathrm{Mol}}$. Therefore, we denote the calculated α^{Mol} in the conventional cluster model as α^{Loc} defined above. The calculated molecular polarizabilities α^{Loc} of adsorbed pyridine and benzene systems are listed in Table S1. For example, α_{xx} in the Py-Au_7 cluster model is calculated to be 285.85 a_0^3, while $\frac{\partial^2 E_{\mathrm{Metal}}}{\partial F_a \partial F_b}$ and $\frac{\partial^2 E_{\mathrm{Mol}}}{\partial F_a \partial F_b}$ are calculated to be 250.97 and 40.711 a_0^3, respectively. Hence we can deduce the interaction contribution in α_{xx} as 285.85 – (250.97 + 40.711) = -5.831 a_0^3.

Table S1 Calculated matrix elements of polarizabilities in a_0^3 for pyridine or benzene adsorbed on coinage metal substrates: Py or Ben-Metal $\left(\frac{\partial^2 E(tot)}{\partial F_a \partial F_b}\right)$, metal $\left(\frac{\partial^2 E_{\text{Metal}}}{\partial F_a \partial F_b}\right)$, Py or Ben $\left(\frac{\partial^2 E_{\text{Mol}}}{\partial F_a \partial F_b}\right)$, and Py or Ben $\left(\alpha^{Loc}\right)$ at the B3LYP/Sadlej pVTZ/Lanl2dz level.

Species	α_{xx}	α_{yx}	α_{yy}	α_{zx}	α_{zy}	α_{zz}
Py-Au_7	285.8500	0.0000	521.6200	0.0000	0.0000	334.0110
Au_7	250.9700	0.0000	463.8330	0.0000	0.0000	178.9580
Py	40.7110	0.0000	79.1800	0.0000	0.0000	74.2380
Py α^{Loc}	37.7955	0.0000	68.4835	0.0000	0.0000	114.6455
Py-Ag_7	395.9560	0.0000	519.6620	0.0000	0.0000	319.9150
Ag_7	367.8720	0.0000	464.6660	0.0000	0.0000	189.3360
Py	40.6970	0.0000	79.1290	0.0000	0.0000	74.2700
Py α^{Loc}	34.3905	0.0000	67.0625	0.0000	0.0000	102.4245
Py-Cu_7	373.7020	0.0000	375.6970	0.0000	0.0000	279.8220
Cu_7	340.6370	0.0000	320.7720	0.0000	0.0000	138.3960
Py	40.6980	0.0000	79.1100	0.0000	0.0000	74.2730
Py α^{Loc}	36.8815	0.0000	67.0175	0.0000	0.0000	107.8495
Ben-Au_6	345.7900	0.0000	345.8270	0.0000	0.0150	187.8940
Au_6	291.6980	0.0000	291.6980	0.0000	0.0000	120.8840
Ben	83.3110	0.0000	83.3080	0.0000	0.0000	44.6610
Ben α^{Loc}	68.7015	0.0000	68.7185	0.0000	0.0075	55.8355
Ben-Ag_6	407.8910	0.0000	407.9340	0.0000	-0.0050	208.8480
Ag_6	353.8410	0.0000	353.8350	0.0000	0.0010	142.9280
Ben	83.3350	0.0000	83.3330	0.0000	0.0000	44.6690
Ben α^{Loc}	68.6925	0.0000	68.7160	0.0000	-0.0030	55.2945
Ben-Cu_6	327.3280	0.0000	327.3540	0.0000	-0.0020	188.9510
Cu_6	273.1490	0.0000	273.1440	0.0000	0.0000	118.7970
Ben	83.3140	0.0000	83.3110	0.0000	0.0000	44.6600
Ben α^{Loc}	68.7465	0.0000	68.7605	0.0000	-0.0010	57.4070

Therefore $\alpha_{xx}^{\text{Mol}} = \alpha_{xx}^{Loc}$ is calculated as 40.711 + 0.5 x (-5.831) = 37.7955 a_0^3. For two states model, Jensen *et al.* have proposed a more rigorous way to get α^{Mol} for such systems.[12] However, up to now, there has been no better method that can be easily used in general situation.

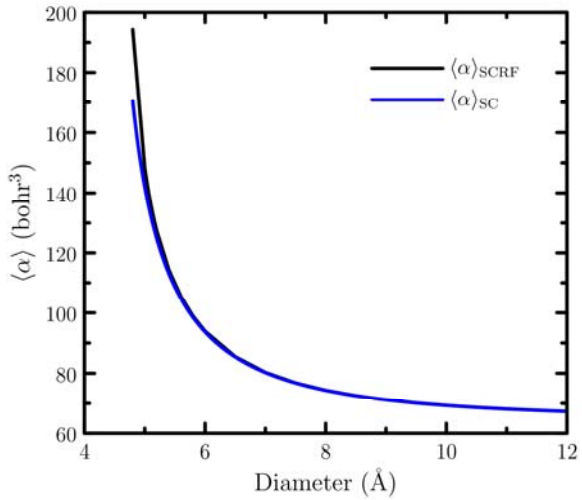

Fig. S2 Calculated average polarizabilities $\langle\alpha\rangle$, i.e. $\frac{1}{3}\left(\alpha_{xx}+\alpha_{yy}+\alpha_{zz}\right)$, of pyridine in a_0^3 at the B3LYP/Sadlej pVTZ level. Comparison between the calculated values from the semi-classic method described in **S1** (blue line) and the exact values from the SCRF method (black line) at different cavity radii. The dielectric constant of the environment is set to be 6.9.

It is possible to consider the surrounding effect with the self-consistent reaction field (SCRF) method within the Onsager model when the molecule examined has a permanent dipole moment. We anticipate that the comparison between the calculated molecular polarizability with the SCRF method and that with the semi-classic method described in **S1** be satisfactory. As a small external electric field has negligible effect on the molecular electronic structure, the molecular electronic structure in the absence of an external electric field is used to calculate the molecular polarizability for this comparison depicted in Fig. S2. Discrepancy between the SCRF and semi-classic polarizabilities of pyridine is indeed small, and that for benzene should be even less than that of pyridine since the dipole moment of an adsorbed benzene is smaller than that of pyridine. These results guarantee that the numerical errors for the derivatives based on Eq. (1.9) be under control.

From Fig. S2 we notice that as the distance between nanoparticles become shorter, the discrepancy of molecular polarizabilities between adsorbed and free molecule becomes larger. According to the well-known Clausius-Mossotti formula[3]

$$\epsilon = \frac{1+\frac{8\pi}{3}N\alpha}{1-\frac{4\pi}{3}N\alpha} \qquad (1.14)$$

the dielectric constant in the "hot-spots" in SERS should be very different from that of the bulk solution. This result indicates that using a uniform dielectric constant in electromagnetic field calculations can be questionable. It also gives a clue to build a nonuniform dielectric constant at the first principles level in

electromagnetic field calculations.

S3 Physical and Chemical Components in the Coupling Enhancement Factor

Logarithm of normal mode independent G_{Coup}^{Phys} calculated by using Eq. (1.6) is plotted in Fig. S3 for pyridine and benzene adsorbed on gold, silver, and copper substrates, respectively. There are two different extrema in Fig. S3 at different distances between nanoparticles. One is the maximum and the other the minimum. This result shows that the electric field of light is first increased by G_{Coup}^{Phys} when the distance between nanoparticles becomes shorter and then decreased when the distance becomes even shorter. This provides an explanation how the adsorbed molecules can tune the surface plasmas, a phenomenon observed in some recent experiments.[13]

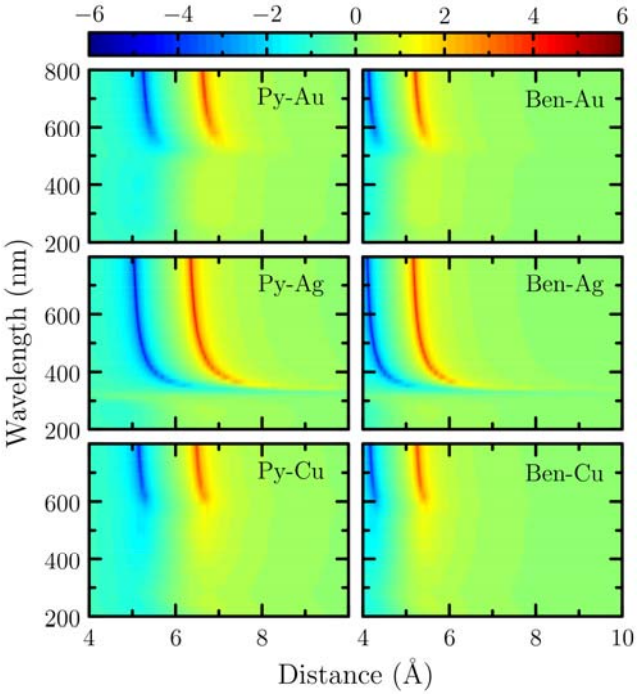

Fig. S3 Logarithm of normal mode independent G_{Coup}^{Phys} for pyridine (left) and benzene (right) adsorbed on gold, silver, and copper substrates from top to bottom. Excitation wavelength from 200 to 800 nm and distance between two nanoparticles from 4 to 10 Å are considered.

In order to discuss the general behavior and the order of magnitude of normal mode dependent G_{Coup}^{Chem}, we have selected the ring breathing mode for pyridine or benzene adsorbed on gold, silver, and copper substrates. We plot logarithm in Fig. S4 for all calculated G_{Coup}^{Chem} of this normal mode for these systems by using Eq. (1.10). From Fig. S4, we can see that, at certain distance between two nanoparticles, G_{Coup}^{Chem} can become as large as 10^6 for both chemical (Py) and physical (Ben) adsorption systems. When molecules are chemically adsorbed on metal surfaces, the distance where G_{Coup}^{Chem} becomes important is longer than that in physisorption. Usually space occupied by molecule in physisorption is larger than that in chemisorption. Hence chemical coupling enhancement factor should play a more important role in chemisorption for SERS. In most situations, G_{Coup}^{Chem} is larger than 1 and Raman intensity is generally increased by this factor.

The distance between nanoparticles where the G_{Coup}^{Phys} maximum appears in chemisorption is longer than that in physisorption. As a result, SERS signals would be easier to be observed in chemisorption than they are in physisorption. This trend is in agreement with the experimental observation.[14] This reveals that physical enhancement dominates at larger distances between nanoparticles while at smaller distances chemical enhancement comes into play. We also notice that in the ultraviolet region of incident light, both G_{Coup}^{Phys} and G_{Coup}^{Chem} become less important. This should be attributed to interband transition of metal.[4]

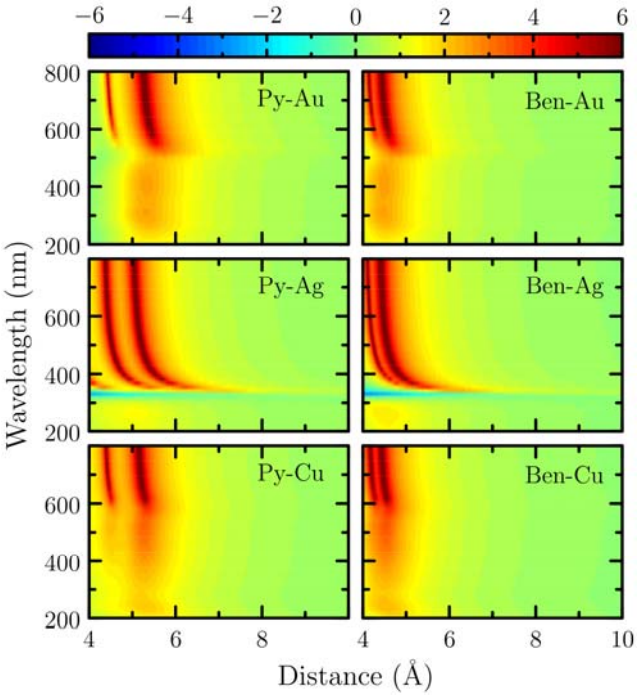

Fig. S4 Logarithm of G_{Coup}^{Chem} for ring breathing mode of pyridine (left) and benzene (right) adsorbed on gold, silver, and copper substrates from top to bottom. Excitation wavelength from 200 to 800 nm and distance between two nanoparticles from 4 to 10 Å are considered.

Notes and references

1. Y. Luo, P. Norman, P. Macak and H. Agren, *J. Phys. Chem. A*, 2000, **104**, 4718-4722.
2. P. Macak, P. Norman, Y. Luo and H. Agren, *J. Chem. Phys.*, 2000, **112**, 1868-1875.
3. C. J. F. Bottcher, *Theory of Electric Polarization*, Elsevier: Amsterdam, 1973.
4. P. B. Johnson and R. W. Christy, *Phys. Rev. B*, 1972, **6**, 4370-4379.

5. J. Neugebauer, C. K. M. Reiher and B. A. Hess, *J. Comput. Chem.*, 2002, **23**, 895-910.
6. A. Bilic, J. R. Reimers and N. S. Hush, *J. Phys. Chem. B*, 2002, **106**, 6740-6747.
7. A. Bilic, J. R. Reimers, N. S. Hush, R. C. Hoft and M. J. Ford, *J. Chem. Theory Comput.*, 2006, **2**, 1093-1105.
8. A. J. Sadlej, *Collect. Czech. Chem. Commun.*, 1988, **53**, 1995-2016.
9. M. J. Frisch, G. W. Trucks, H. B. Schlegel, G. E. Scuseria, M. A. Robb, J. R. Cheeseman, Montgomery, Jr., J. A., T. Vreven, K. N. Kudin, J. C. Burant, J. M. Millam, S. S. Iyengar, J. Tomasi, V. Barone, B. Mennucci, M. Cossi, G. Scalmani, N. Rega, G. A. Petersson, H. Nakatsuji, M. Hada, M. Ehara, K. Toyota, R. Fukuda, J. Hasegawa, M. Ishida, T. Nakajima, Y. Honda, O. Kitao, H. Nakai, M. Klene, X. Li, J. E. Knox, H. P. Hratchian, J. B. Cross, V. Bakken, C. Adamo, J. Jaramillo, R. Gomperts, R. E. Stratmann, O. Yazyev, A. J. Austin, R. Cammi, C. Pomelli, J. W. Ochterski, P. Y. Ayala, K. Morokuma, G. A. Voth, P. Salvador, J. J. Dannenberg, V. G. Zakrzewski, S. Dapprich, A. D. Daniels, M. C. Strain, O. Farkas, D. K. Malick, A. D. Rabuck, K. Raghavachari, J. B. Foresman, J. V. Ortiz, Q. Cui, A. G. Baboul, S. Clifford, J. Cioslowski, B. B. Stefanov, G. Liu, A. Liashenko, P. Piskorz, I. Komaromi, R. L. Martin, D. J. Fox, T. Keith, M. A. Al-Laham, C. Y. Peng, A. Nanayakkara, M. Challacombe, P. M. W. Gill, B. Johnson, W. Chen, M. W. Wong, C. Gonzalez and J. A. Pople, Gaussian, Inc., Wallingford, CT, 2004.
10. L. Zhao, L. Jensen and G. C. Schatz, *J. Am. Chem. Soc.*, 2006, **128**, 2911-2919.
11. W. Koch and M. C. Holthausen, *A Chemist's Guide to Density Functional Theory*, Wiley-VCH Verlag GmbH, 2001.
12. S. M. Morton and L. Jensen, *J. Am. Chem. Soc.*, 2009, **131**, 4090-4098.
13. W. Ni, T. Ambjornsson, S. P. Apell, H. Chen and J. Wang, *Nano Lett.*, 2010, **10**, 77-84.
14. Z. Q. Tian, R. Bin and D. Y. Wu, *J. Phys. Chem. B*, 2002, **106**, 9463-9483.